

A new species of mud snake (Squamata: Homalopsidae: *Myrrophis*) from southern Vietnam

Sang Ngoc Nguyen^{1,2}, Manh Van Le¹, Amy Lathrop³, Thi-Dieu-Hien Vo⁴, Robert W. Murphy⁵, Jing Che^{6,7}

1 Institute of Tropical Biology, Vietnam Academy of Science and Technology, 85 Tran Quoc Toan St., Dist. 3, Ho Chi Minh City, Vietnam

2 Graduate University of Science and Technology, Vietnam Academy of Science and Technology, 18 Hoang Quoc Viet Road, Hanoi, Vietnam

3 Royal Ontario Museum, Department of Natural History, 100 Queen's Park, Toronto, Ontario M5S2C6, Canada

4 Faculty of Environmental and Food Engineering, Nguyen Tat Thanh University, Ho Chi Minh City, Vietnam

5 Reptilia Zoo and Education Centre, 2501 Rutherford Rd Vaughan, Ontario L4K 2N6, Canada

6 State Key Laboratory of Genetic Resources and Evolution & Yunnan Key Laboratory of Biodiversity and Ecological Conservation of Gaoligong Mountain, Kunming Institute of Zoology, Chinese Academy of Sciences, Kunming 650223, China

7 Southeast Asia Biodiversity Research Institute, Chinese Academy of Sciences, Yezin, Nay Pyi Taw 05282, Myanmar

<https://zoobank.org/AF7CD34B-81DC-485F-BD2B-D36F7BB08A81>

Corresponding authors: Sang Ngoc Nguyen (ngocsangitb@yahoo.com), Jing Che (chej@mail.kiz.ac.cn)

Academic editor Uwe Fritz | Received 7 December 2023 | Accepted 8 February 2024 | Published 11 March 2024

Citation: Nguyen SN, Le MV, Lathrop A, Vo T-D-H, Murphy RW, Che J (2024) A new species of mud snake (Squamata: Homalopsidae: *Myrrophis*) from southern Vietnam. Vertebrate Zoology 74 221–233. <https://doi.org/10.3897/vz.74.e116992>

Abstract

Homalopsid snakes of the genus *Myrrophis* include only two species distributed in southern China and northern Vietnam. Here, we describe a third species from southern Vietnam based on morphological data and nucleotide sequences from the mitochondrial gene *cyt b*. *Myrrophis dakkrongensis sp. nov.* is diagnosed by the following morphological characters: Medium-sized mud snake (largest total length 452 mm); internasal single and distinctly separated from loreals; dorsal scales smooth, in 23 rows at midbody, reduced to 19 or 20 rows before vent; ventrals 133–138; subcaudals 34–42, paired; cloacal plate divided; supralabials 8, fourth entering orbit; second pair of chin-shields small and oblique; maxillary teeth 17 or 18; gland-like tubercles present in the cloacal region; hemipenis short, forked and spinose, reaching 7th subcaudal; dorsum dark brown to black; and a white or yellow to orange lateroventral stripe present. The new species differs from its congeners by an uncorrected *p* distance in *cyt b* sequences of at least 10.5%.

Key words

Dak Nong Province, *Gyiophis*, hemipenis, Mekong River, mitochondrial DNA, *Myanophis*, *Myrrophis bennettii*, *Myrrophis chinensis*, *Myrrophis dakkrongensis*

Introduction

Homalopsid snakes of the family Homalopsidae occur in the Asian-Australopapuan region and have the following characters: (1) hypapophyses present along the length of the vertebral column; (2) hemipenis forked, with shal-

low cups and distal end finely calyculate, spines present and variable in size; (3) tracheal lung present; (4) crescent-shaped valvular nare; (5) shallow rostral notch; (6) elliptical pupil; (7) subcaudals and cloacal plate divided;

and (8) viviparous with a placenta-like connection to the female's circulatory system (Murphy and Voris 2014). They are aquatic or semi-aquatic, and several species can inhabit brackish water or the sea. In rear-fanged homalopsids, the anterodorsal position of the nostrils enables them to breathe by raising only a small part of their heads out of the water (Gyi 1970). Gyi (1970) arranged the 34 species known at that time into ten genera and gave detailed descriptions for each genus and species. Murphy and Voris (2014) carefully revised the family and divided the 53 homalopsids into 28 genera, of which five genera were new. Since the comprehensive work of Murphy and Voris (2014), four new homalopsids have been discovered and an additional new genus erected (Köhler et al. 2021; Uetz et al. 2023). Currently, the family has 57 species belonging to 29 genera (Uetz et al. 2023).

The genus *Myrophis* Kumar, George, Sanders & Murphy was erected in 2012 for two species, *M. bennettii* (Gray, 1842) and *M. chinensis* (Gray, 1842) (Kumar et al. 2012). Morphologically, the species of *Myrophis* differ from other homalopsids by a combination of the following characters: Dorsal scales smooth, nasals in contact, 21–23 dorsal scale rows at mid-body, internasal not in contact with the loreal, five lower labials contact first chin shield, and some dorsal scales in the cloacal region have enlarged, gland-like tubercles (Kumar et al. 2012; Murphy and Voris 2014). *Myrophis* exists in southern China and northern Vietnam (Zhao 2006; Kumar et al. 2012; Huang 2021).

During our fieldwork in Dak Nong Province, southern Vietnam from 1 to 13 August 2018, we collected three specimens of *Myrophis* that were morphologically similar to *M. chinensis*. However, detailed analyses of scale characters and mitochondrial DNA sequences showed that they differed morphologically and genetically from *M. chinensis*. Analyses of DNA and morphology also failed to assign them to the other congener, *M. bennettii*. Hence, below we describe the three specimens as a new species.

Material and methods

All specimens were collected by hand or by fishing net in Quang Son Commune, Dak Glong District, Dak Nong Province, Vietnam. Specimens were euthanized by using ethyl acetate (Simmons 2002), fixed in 90% ethanol, and subsequently transferred to 70% ethanol for storage in the Institute of Tropical Biology Collection of Zoology (ITBCZ), Ho Chi Minh City, Vietnam. Hemipenes were forcibly everted by injecting water directly into the tail base of freshly killed specimens. Terminology for hemipenis follows Dowling and Savage (1960), Smith (1943), and Gyi (1970). Maxillary teeth were counted by removing a maxillary bone from the specimen and observing under a zoom stereo microscope (Akeiyo, Hong Kong) at 7X–45X.

Morphological analysis

Morphological characters taken from Gyi (1970), Murphy (2007), Murphy and Voris (2014), and Quah et al. (2017) were recorded as follows:

Measurements: snout to vent length: measured from the tip of the snout to the vent; tail length: measured from the vent to the tip of the tail; total length: sum of snout–vent length and tail length; rostral width: greatest width of rostral; rostral height: greatest height of rostral; nasal width: greatest width of nasal; nasal length: greatest length of nasal; internasal width: greatest width of internasal; internasal length: greatest length of internasal; prefrontals width: width of the two prefrontals; prefrontals length: length of prefrontals along their median suture; frontal width: width of frontal at the broadest point; frontal length: length of frontal along middorsal line; frontal–snout distance: distance from the anterior margin of the frontal to the tip of the snout. The following scale dimensions were measured regardless of scale shape: parietal length: greatest length of parietal; loreal height: greatest height of loreal; loreal length: greatest length of loreal; anterior chin shield length: greatest length of anterior chin shield; anterior chin shield width: greatest width of anterior chin shield; posterior chin shield length: greatest length of posterior chin shield; posterior chin shield width: greatest width of posterior chin shield.

Scale counts: supralabials; infralabials; loreals; preoculars; postoculars; anterior temporals; posterior temporals; dorsal scales at the first ventral: starting from the dorsal scale adjacent to the first complete ventral and counting obliquely backward to the vertebral row and then forward to the dorsal scale adjacent to the first ventral on the other side of the body; dorsal scales at neck: number of dorsal scale rows at one head length behind the head; dorsal scales at midbody: counted half-way between the first ventral and the vent, counting obliquely forward and turning backward at the vertebral row; dorsal scales at the third ventral anterior to the vent: counted at the level equal to the third from the last ventral, counting obliquely forward and turning backward at the vertebral row; dorsal scales before vent: number of dorsal scale rows at one head length prior to the vent; ventral scales: count according to Dowling (1951) and the cloacal plate was not included in the number of ventrals; preventrals: incomplete ventrals that wider than long but not in contact with the first dorsal scale rows simultaneously on both sides; subcaudal scales: number of subcaudal scales, excluding the terminal spine.

In addition, the following characters were also obtained: number of maxillary teeth; supralabial entering the orbit; internasal and loreal in contact or separated; number of infralabials in contact with the anterior chin shield; cloacal plate single or divided; hemipenis length: length that the hemipenes extend in terms of numbers of subcaudal scales; gland-like tubercles: number of enlarged, gland-like tubercles in the cloacal region; central spot on each ventral present or absent; lateroventral stripe present or absent.

Values of paired characters are given in order of left/right. Measurements (in millimeters), except for snout-vent length and tail length, were taken with digital calipers (Exploit 150 mm, China) to the nearest 0.1 mm using a zoom stereo microscope at 7X–45X.

For comparison, morphological characters of species of *Myrophis* were taken from the literature (Boulenger 1896; Pope 1935; Bourret 1936; Smith 1943; Kumar et al. 2012; Murphy and Voris 2014; Köhler et al. 2021) and examined specimens (Appendix 1).

DNA analysis

Liver samples from the three individuals were preserved in absolute ethanol and kept at -20°C. Total genomic DNA was extracted using DNeasy Blood and Tissue Kit (Qiagen, Germany), following protocols by the manufacturer's instructions. A fragment of mitochondrial gene

encoding cytochrome *b* (cyt *b*) was sequenced in both directions. PCR was performed using HotStar Taq Mastermix (Qiagen, Germany). Primers used for PCR and sequencing were L14910 (5'- GAC CTG TGA TMT GAA AAC CAY CGT TGT -3') and H16064 (5'- CTT TGG TTT ACA AGA ACA ATG CTT TA -3') (Indahsari et al. 2019). The PCR volume consisted of 21 μ l (2 μ l each primer, 5 μ l water, 10 μ l of Taq mastermix and 1–2 μ l of DNA depending on the quality of DNA in the final extraction solution). PCR conditions were performed as follows: Initial denaturation step at 95°C for 15min; followed by 35 cycles of denaturation at 95°C for 30s, annealing at 48°C for 45s, and extension at 72°C for 1min; and a final elongation step at 72°C for 6min. PCR products then were visualized using electrophoresis through a 1% agarose gel, marker 1kb, 1X TBE and stained with ethidium bromide and photographed under UV light. Successful amplifications were purified using GeneJet PCR Purification Kit (ThermoFisher Scientific, Lithuania). Cleaned

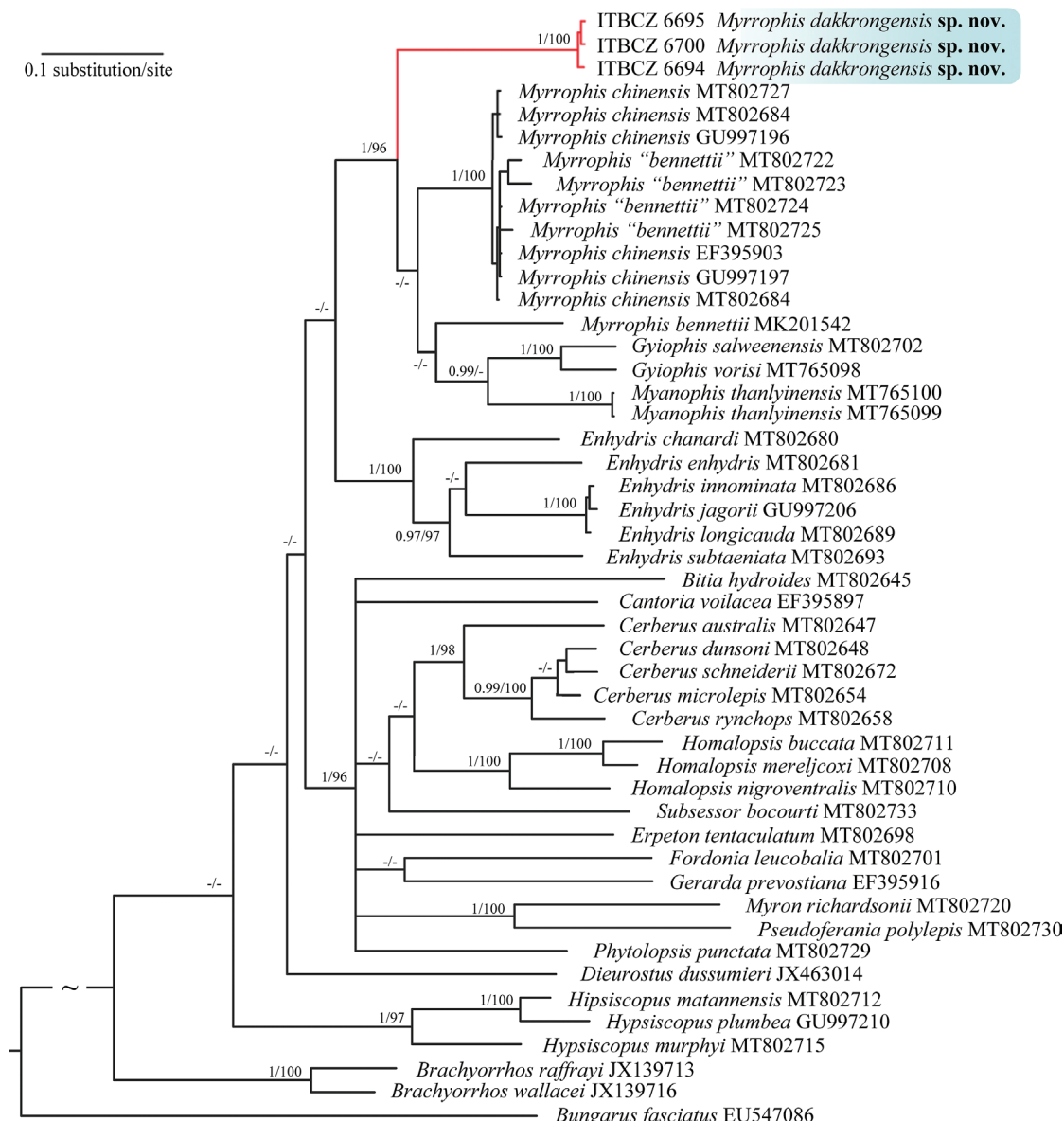


Figure 1. The Bayesian inference (BI) tree reconstructed from the *cyt b* gene for homalopsid species. Branch support values from BI and Maximum Likelihood (ML), respectively (BI/ML). A hyphen indicates an un-supported node.

Table 1. List of samples of homalopsid snakes used for molecular analyses in this study.

Species	Voucher	GenBank Accession No. (cyt b)	Locality	Reference
<i>Myrophis dakkrongensis</i> sp. nov.	ITBCZ 6694	PP214982	Dak Glong, Dak Nong Prov., Vietnam	This study
<i>Myrophis dakkrongensis</i> sp. nov.	ITBCZ 6695	PP214980	Dak Glong, Dak Nong Prov., Vietnam	This study
<i>Myrophis dakkrongensis</i> sp. nov.	ITBCZ 6700	PP214981	Dak Glong, Dak Nong Prov., Vietnam	This study
<i>Bitia hydroides</i>	LSUHC 10516	MT802645	Penang, Malaysia	Bernstein et al. (2021)
<i>Brachyorrhos raffrayi</i>	MZB 4009	MT139713	Ternate, Indonesia	Murphy et al. (2012)
<i>Brachyorrhos wallacei</i>	MZB 3463	MT139716	Halmahera, Indonesia	Murphy et al. (2012)
<i>Cantoria violacea</i>	FMNH 250117	EF395897	Phuket, Thailand	Alfaro et al. (2008)
<i>Cerberus australis</i>	MAGNT 29853	MT802647	Darwin, Australia	Bernstein et al. (2021)
<i>Cerberus dunsoni</i>	CAS 236318	MT802648	Palau, Philippines	Bernstein et al. (2021)
<i>Cerberus microlepis</i>	USMN 579917	MT802654	Camarines Sur, Philippines	Bernstein et al. (2021)
<i>Cerberus rynchops</i>	CAS 222968	MT802658	Rakhine, Myanmar	Bernstein et al. (2021)
<i>Cerberus schneiderii</i>	NCSM 99001	MT802672	Kampot, Cambodia	Bernstein et al. (2021)
<i>Dieurostus dussumieri</i>	SAMA: ABTC 149492	JX463014	Kerala, India	Kumar et al. (2012)
<i>Enhydris chanardi</i>	YPM 15037	MT802680	Pet trade	Bernstein et al. (2021)
<i>Enhydris enhydris</i>	FMNH 259100	MT802681	Kien Giang, Vietnam	Bernstein et al. (2021)
<i>Enhydris innominata</i>	FMNH 259250	MT802686	Kien Giang, Vietnam	Bernstein et al. (2021)
<i>Enhydris jagorii</i>	THNHM 12164	GU997206	Uttaradit, Thailand	Karns et al. (2010)
<i>Enhydris longicauda</i>	FMNH 257254	MT802689	Siem Reap, Cambodia	Bernstein et al. (2021)
<i>Enhydris subtaeniata</i>	FMNH 259086	MT802693	Kien Giang, Vietnam	Bernstein et al. (2021)
<i>Erpeton tentaculatum</i>	FMNH 259080	MT802698	Kien Giang, Vietnam	Bernstein et al. (2021)
<i>Fordonia leucobalia</i>	SAMA: ABTC 55470	MT802701	Northern Territory, Australia	Bernstein et al. (2021)
<i>Gerarda prevostiana</i>	ZRC2.346	EF395916	Lim Chu Kang, Singapore	Alfaro et al. (2008)
<i>Gyiophis salweenensis</i>	LSUHC 12960	MT802702	Kayin, Myanmar	Bernstein et al. (2021)
<i>Gyiophis vorisi</i>	SMF 100700	MT765098	Myanmar	Köhler et al. (2021)
<i>Homalopsis buccata</i>	LSUHC 10349	MT802711	Penang, Malaysia	Bernstein et al. (2021)
<i>Homalopsis mereljcoxi</i>	FMNH 259088	MT802708	Kien Giang, Vietnam	Bernstein et al. (2021)
<i>Homalopsis nigroventralis</i>	NCSM 76560	MT802710	Savannakhet, Laos	Bernstein et al. (2021)
<i>Hypsiscopus matannensis</i>	MVZ 239382	MT802712	Sulawesi, Indonesia	Bernstein et al. (2021)
<i>Hypsiscopus murphyi</i>	FMNH 259225	MT802715	Vientiane, Laos	Bernstein et al. (2021)
<i>Hypsiscopus plumbea</i>	FMNH 263707	GU997210	Prachan Takam, Thailand	Karns et al. (2010)
<i>Myanophis thanlynensis</i>	SMF 100707	MT765099	Yangon, Myanmar	Köhler et al. (2021)
<i>Myanophis thanlynensis</i>	SMF 100709	MT765100	Yangon, Myanmar	Köhler et al. (2021)
<i>Myron richardsonii</i>	SAMA: ABTC 55494	MT802720	Northern Territory, Australia	Bernstein et al. (2021)
<i>Myrophis "bennettii"</i>	MVZ 224179	MT802722	Vinh Phuc Prov., Vietnam	Bernstein et al. (2021)
<i>Myrophis "bennettii"</i>	MVZ 224180	MT802723	Vinh Phuc Prov., Vietnam	Bernstein et al. (2021)
<i>Myrophis "bennettii"</i>	MVZ 224183	MT802724	Vinh Phuc Prov., Vietnam	Bernstein et al. (2021)
<i>Myrophis "bennettii"</i>	MVZ 224184	MT802725	Vinh Phuc Prov., Vietnam	Bernstein et al. (2021)
<i>Myrophis bennettii</i>	CHS 807	MK201542	Guangdong, China	Li et al. (2020)
<i>Myrophis chinensis</i>	ROM 30889	GU997196	Tam Dao, Vinh Phuc Prov., Vietnam	Karns et al. (2010)
<i>Myrophis chinensis</i>	ROM 30890	GU997197	Tam Dao, Vinh Phuc Prov., Vietnam	Karns et al. (2010)
<i>Myrophis chinensis</i>	ROM 31031	EF395903	Tam Dao, Vinh Phuc Prov., Vietnam	Alfaro et al. (2008)
<i>Myrophis chinensis</i>	AMNH 106675	MT802726	Vietnam	Bernstein et al. (2021)
<i>Myrophis chinensis</i>	LSUHC 4255	MT802727	Hainan, China	Bernstein et al. (2021)
<i>Myrophis chinensis</i>	ROM 25620	MT802684	Hanoi, Vietnam	Bernstein et al. (2021)
<i>Phytolopsis punctata</i>	FMNH 250112	MT802729	Selangor, Malaysia	Bernstein et al. (2021)
<i>Pseudoferania polylepis</i>	BPBM: 43422	MT802730	Papua, Indonesia	Bernstein et al. (2021)
<i>Subsessor bocourti</i>	FMNH 257251	MT802733	Siem Reap, Cambodia	Bernstein et al. (2021)

PCR products were sent to First Base (Malaysia) for sequencing using Sanger method.

New nucleotide sequences of cyt *b* were manually verified using SeqMan (DNASTAR Lasergene 7, Madison, WI) and then combined with available homalopsid sequences selected from GenBank. Obtained sequences were then aligned using ClustalW (Thompson et al. 1994)

integrated in MEGA5 (Tamura et al. 2011) with default parameters. Uncorrected inter- and intraspecific p distances were calculated using MEGA5. The cyt *b* dataset consisted of 47 ingroup samples including our three new sequences and 44 published sequences selected from Li et al. (2020), Bernstein et al. (2021), and Köhler et al. (2021), which cover 34 homalopsid species of 17 genera (Table 1).

Defining sequences MT802722–5 as *Myrrophis bennetti* (Bernstein et al. 2021) may be a case of misidentification (see Discussion) and we therefore put the name in quotes (*Myrrophis “bennetti”*). *Bungarus fasciatus* (Schneider, 1801) (GenBank accession number EU547086) was used as the outgroup taxon based on Bernstein et al. (2021).

Phylogenetic trees from cyt *b* sequences were constructed using Bayesian Inference (BI) and Maximum Likelihood (ML) approaches. The best-fit evolutionary model used for BI was GTR+I+G as selected by MrModeltest v2.3 (Nylander 2004) under the Akaike Information Criterion. BI was performed in MrBayes v3.1.2 (Ronquist and Hulsenbeck 2003). Bayesian posterior probabilities (BPP) were estimated using a Markov chain Monte Carlo sampling approach with 1,200,000 generations, saving one tree every 100 generations. The runs were stopped when the average standard deviations reached 0.0085. The initial 25% of the samples were discarded as burn-in. The remaining trees were combined, and a 50% majority consensus tree was generated. ML analysis was implemented in the IQ-TREE webserver (Nguyen et al. 2015; Trifinopoulos et al. 2016) using the substitution model selected above. One-thousand bootstrap pseudoreplicates via the ultrafast bootstrap (UFB; Hoang et al. 2018) approximation algorithm were employed. We considered nodes having BPP of $\geq 95\%$ and UFB of $\geq 95\%$ as being strongly supported (Hillis and Bull 1993; Minh et al. 2013). The resulting trees were visualized in FigTree v1.4.3 (<http://tree.bio.ed.ac.uk/software/figtree>) and rooted based on the above outgroup.

Results

Sequence variation and genetic distances

We obtained 1047 bp of cyt *b* for the three individuals of our mud snake, which were deposited in GenBank (Table 1). The final matrix of cyt *b* consisted of 48 sequences with 460 potentially parsimony-informative characters.

The uncorrected interspecific p distances in cyt *b* between our mud snakes and other homalopsid species ranged from 10.5% (vs. *Myrrophis “bennetti”*) to 21.3% (vs. *Cantoria violacea*), averaging $17.3 \pm 3.0\%$ (Table 2). *Myrrophis chinensis* differed from *M. “bennetti”* by only 0.2% but differed from *M. bennetti* by 10.1%. *Gyiophis salweenensis* differed from *G. vorisi* by 6.3% (Table 2). Interspecific p distance between three individuals of our mud snakes averaged 0.5%.

Phylogenetic trees

The BI and ML trees reconstructed from cyt *b* sequences were similar to each other in topology and differed only in their resolution of poorly supported nodes. Only the 50% majority rule consensus tree from the BI analysis is shown in Figure 1, but with branch support values from

Table 2. Average uncorrected p distance (%) in cyt *b* between species on the *Gyiophis-Myanophis-Myrrophis* clade showed in Figure 1.

	Taxon	1	2	3	4	5	6
1	<i>Myrrophis dakkrongensis</i> sp. nov.						
2	<i>Gyiophis salweenensis</i>	14.2					
3	<i>Gyiophis vorisi</i>	13.5	6.3				
4	<i>Myanophis thanlyinensis</i>	15.5	13.2	13.2			
5	<i>Myrrophis “bennetti”</i>	10.5	9.8	10.8	10.6		
6	<i>Myrrophis bennetti</i>	15.0	12.8	13.2	12.8	10.1	
7	<i>Myrrophis chinensis</i>	10.9	10.2	10.8	10.3	0.2	10.1

both BI and ML. Accordingly, all analyzed homalopsid species formed six main clades with strong support by both BI and ML analyses. Snakes in the genera *Brachyorrhos*, *Dieurostus*, and *Hypsiscopus* formed three independent lineages corresponding to each genus. The fourth main clade included species in *Bitia*, *Cantoria*, *Cerberus*, *Erpeton*, *Fordonia*, *Gerarda*, *Homalopsis*, *Myron*, *Phytolopsis*, *Pseudoferaania*, and *Rynchops*, with strong support by BI (BPP = 1.00) and ML (UFB = 96%). The fifth main clade consisted of all members in the genus *Enhydris* with full support from both analyses. Our new samples clustered into the sixth main clade together with species in genera *Gyiophis* (2 species), *Myanophis* (monotypic), and *Myrrophis* (2 species), with strong support by BI (BPP = 1.00) and ML (UFP = 96%). These three samples formed an independent clade with full support from both analyses. Because our new snakes differed morphologically and genetically from other homalopsids, we describe them as a new species.

Myrrophis dakkrongensis sp. nov.

<https://zoobank.org/B58E6FB7-E25B-433F-8CBA-4E76405F371B>

Holotype. ITBCZ 6695, adult male, collected from Quang Son, Dak Glong District, Dak Nong Province, Vietnam; coordinates $12^{\circ}10'24''$ N, $107^{\circ}46'36''$ E; elevation 890 m a.s.l. by Sang N. Nguyen, on 3 August 2018 (Figs 2, 3, 5).

Paratypes. Two specimens: ITBCZ 6694 (gravid female) and ITBCZ 6700 (adult male), also collected from Quang Son by the same collector. The former was collected on 2 August 2018 at coordinates $12^{\circ}10'22''$ N, $107^{\circ}46'20''$ E and elevation 890 m a.s.l. The latter was collected on 12 August 2018 at coordinates $12^{\circ}09'22''$ N, $107^{\circ}46'56''$ E and elevation 870 m a.s.l. (Figs 4, 5).

Diagnosis. *Myrrophis dakkrongensis* sp. nov. is distinguished from all of its congeners by the unique combination of the following morphological characters: medium-sized mud snake (largest TL 452 mm in adult female); internasal single and not in contact with loreals; dorsal scale rows 23–23–19 or 23–23–20, smooth; tail short (TaL/



Figure 2. Holotype of *Myrrophis dakkrongensis* sp. nov. (ITBCZ 6695) in life.



Figure 3. Holotype of *Myrrophis dakkrongensis* sp. nov. (ITBCZ 6695). A–C Dorsal, ventral, and lateral views of head, respectively; D ventral view; E cloacal region showing three yellow gland-like tubercles on both sides; F lateral view of right maxillary teeth.



Figure 4. Paratypes of *Myrrophis dakkrongensis* sp. nov. and habitats of the new species. **A** Paratype ITBCZ 6694; **B, C** paratype ITBCZ 6700 and its hemipenes; **D** rubber plantation where the holotype was collected; **E** wetland in forest where paratype ITBCZ 6700 was collected.

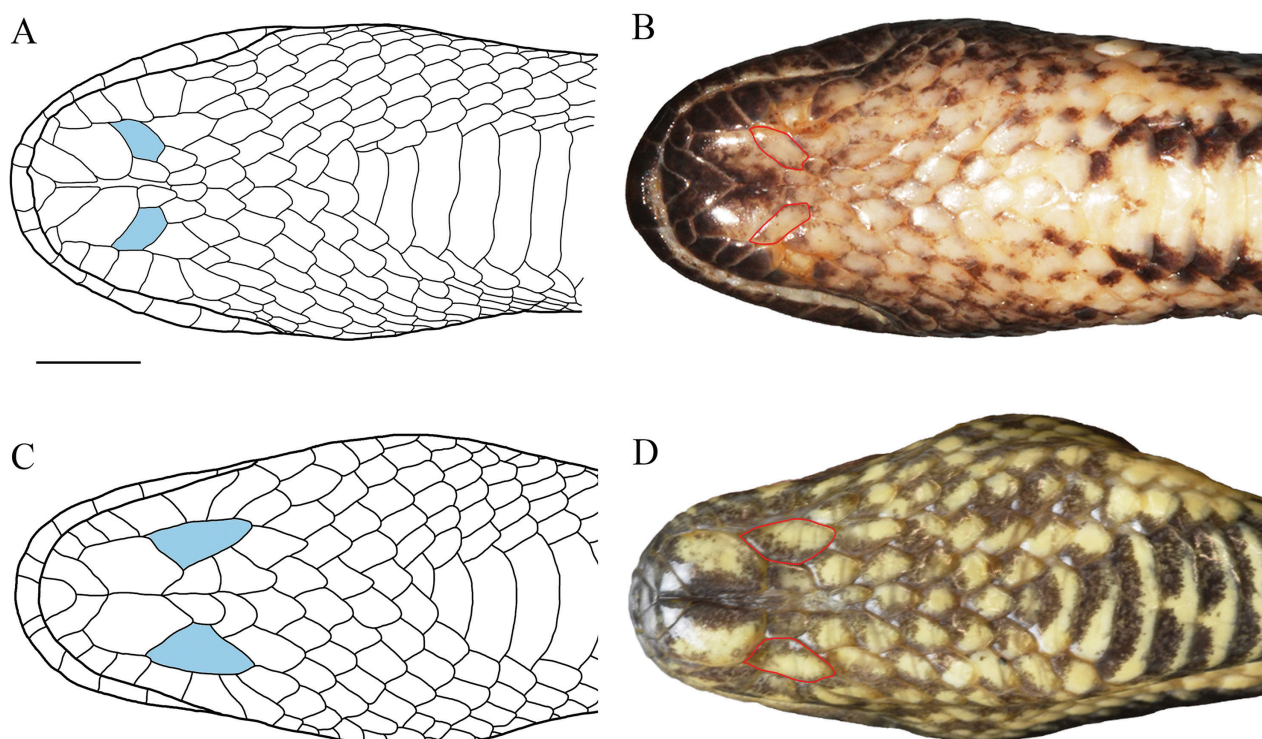


Figure 5. Ventral view of heads of *Myrrophis dakkrongensis* sp. nov. (**A, B**) and *Myrrophis chinensis* (**C, D**) showing difference in the second pair of chin shields (highlighted). **A** Line drawing of head of the holotype ITBCZ 6695; **B** paratype ITBCZ 6700; **C** line drawing of head of *Myrrophis chinensis* (re-drawn from Boulenger 1896); **D** examined specimen ROM 31031. Scale bar 5 mm.

TL ratio 0.15–0.16 in males and 0.14 in female); ventrals 134–138 in males and 133 in female; subcaudals 39–42 in males and 34 in female; 8 supralabials, fourth entering orbit; second pair of chin-shield small, oblique, and in contact with two infralabials; 17 or 18 maxillary teeth; hemipenis short, forked and spinose, reaching 7th subcaudal; cloacal plate divided; gland-like tubercles present in the cloacal region; dorsum dark brown to black; and white or yellow to orange lateroventral stripe present.

Description of holotype. Adult male; head elliptical in dorsal view, slightly distinct from neck; body short and cylindrical; SVL 372 mm; tail 70 mm (TaL/TL = 0.16); eye small, pupil vertically elliptical to round, situated on latero-dorsal side of the head; nostril directed upward.

Dorsal head scales smooth, slightly overlapping (Fig. 3A); rostral broader than high (width 3.6 mm, height 1.8 mm), narrowly visible from above, touching nasals and 1st supralabial on both sides; nasals enlarged, more or less pentagonal, broadly in contact with one another behind the rostral; lateral nasal cleft distinctly sunken and extending to first labial, posterior nasal cleft shallow and extending to internasal; internasal single, lozenge-shaped, broader than long (width 2.5 mm, length 2.1 mm), not in contact with loreals; prefrontals forming median suture, in broad contact with nasals; frontal elongated, shield-shaped, almost twice as long as broad (width 2.6 mm, length 5.0 mm), almost as long as distance from tip of snout, and shorter than parietals; parietals in contact with each other behind frontal, each bordered laterally by upper temporals and anteriorly by frontal, supraocular and upper postocular; loreal single, longer than high and in contact with three first supralabials; preocular 1/1; postoculars 2/2, upper higher than long, lower longer than high; anterior temporal 1/1, posterior temporals 2/2, tertiary temporals 3/3; supralabials 8/8, 4th bordering eye, 4th–7th largest, 8th smallest; infralabials 11/11, first pair medially in contact with each other, first four in contact with anterior chin-shield, 4th and 5th in contact with posterior chin-shield, 6th largest; anterior chin shields much longer and wider than posterior ones (length 3.9 mm vs. 2.5 mm, width 1.8 mm vs. 1.1 mm), anterior pair in contact with each other; posterior pair small, oblique, separated from each other by two small scales, and in contact with two infralabials (Figs 3B, 5A); six gulars and two preventrals between anterior chin-shield and 1st ventral.

Dorsal scales smooth, in 27 rows at first ventral, 23 rows at one head length behind head, 23 rows at midbody, 20 rows at one head length prior to vent, and 19 rows at third ventral anterior to vent; vertebral scale row same size and shape as other dorsal scales; dorsal scale row reduction from 23 to 21 at ventrals 87–92 by fusing 4th and 5th rows of body scales on both sides and from 21 to 19 at ventrals 122–126; ventrals 134 (plus two preventrals), broad, not keeled; cloacal plate divided; three gland-like tubercles on lateral sides of cloacal region (Fig. 3E); subcaudals 42, all paired; terminal caudal scale forming a pointed cap.

Maxillary teeth 17, forming two groups separated by small diastema: anterior group with 15 teeth, strongly re-

flected backward; posterior group with two grooved teeth (Fig. 3F).

Hemipenis short and spinose, extending to 8th subcaudal and forked at 4th subcaudal, having three main distinct areas: basal part naked, median part with enlarged curved spines, and distal part with two lobes bearing small and blunt spines. Bifurcate sulcus spermaticus moderately prominent and divided on two lobes.

In life, dorsal and lateral parts of body and tail dark brown; a distinct yellow to orange lateroventral stripe extending from neck to cloacal region, formed by upper half of first dorsal scale row, second dorsal scale row, and lower half of third dorsal scale row (Figs 2, 3); venter cream to yellowish with three dark brown longitudinal stripes: two outer stripes occupy lower half of first dorsal scale row and outer margin of ventral; middle stripe at the center of each ventral. In preservation, color faded but pattern remains, with dorsal and lateral parts black; all yellow and orange parts becoming white or cream.

Variation. Paratype ITBCZ 6700 has black dorsum and nasal cleft extending to loreal on both sides. Paratype ITBCZ 6694 has grey dorsum, white lateroventral stripe at the upper half of the first dorsal scale row and the lower half of the second dorsal scale row, and black ventral scales with white color on the posterior margin forming two bright longitudinal stripes. The enlarged, gland-like tubercles in cloacal region in this female are indistinct. Little variation occurs in size and scalation of the type series (Table 3).

Sexual dimorphism. Males (n = 2) have marginally longer tails than the female (n = 1) (TaL/TL 0.15–0.16 in males; 0.14 in females) and more subcaudals (SC 39–42 in males, 34 in female). Males have distinct gland-like tubercles on lateral sides of the cloacal region, whereas this character in the sole female is indistinct.

Etymology. The specific epithet *dakkrongensis* is a toponym derived from the Dak Krong River system where the new species was discovered. We recommend “Dak Krong mud snake” and “Rắn bòng đák krông” as the common English and Vietnamese names of the new species, respectively.

Distribution. The new species is currently known only from its type locality in Dak Glong District, Dak Nong Province, Vietnam (Fig. 6).

Field notes. The holotype was collected at night when it was moving on the ground in a rubber plantation after a heavy rain (Fig. 4D). The paratypes were collected in the daytime in a fishing net of local people set in a wetland in forest (Fig. 4E). Paratype ITBCZ 6694 bears 12 well-developed embryos.

Comparisons. *Myrophis dakkrongensis* sp. nov. differs from all species in the family Homalopsidae, except for members in the genus *Myrophis*, by the following unique combination of morphological characters: (1)

Table 3. Morphological characters of the type series of *Myrrophis dakkrongensis* sp. nov. Measurements in millimeters.

Voucher	ITBCZ 6695 Holotype	ITBCZ 6694 Paratype	ITBCZ 6700 Paratype
Sex	Male	Female	Male
Snout to vent length	372	388	356
Tail length	70	64	62
Total length	442	452	418
Tail length/Total length ratio	0.16	0.14	0.15
Rostral width	3.6	4.1	3.4
Rostral height	1.8	2.0	1.7
Nasal width	2.9	3.4	2.3
Nasal length	2.1	4.0	2.8
Internasal width	2.5	3.6	3.4
Internasal length	2.1	2.5	1.9
Prefrontals width	4.7	5.6	5.0
Prefrontals length	1.0	1.4	0.9
Frontal width	2.6	4.1	2.8
Frontal length	5.0	6.7	5.0
Frontal-snout length	4.9	6.9	4.4
Parietal length	5.9	8.8	6.1
Loreal height	1.4	2.2	1.6
Loreal length	1.7	2.4	1.8
Anterior chin shield length	3.9	5.2	3.5
Anterior chin shield width	1.8	3.0	1.8
Posterior chin shield length	2.5	3.1	2.3
Posterior chin shield width	1.1	2.1	0.9
Supralabials	8/8	8/8	8/8
Supralabial entering the orbit	4 th /4 th	4 th /4 th	4 th /4 th
Infralabials	11/11	11/11	11/11
Number of infralabials in contact with the anterior chin shield	4/4	4/4	4/4
Loreal	1	1	1
Relative position between internasal and loreal	Separated	Separated	Separated
Preocular	1/1	1/1	1/1
Postocular	2/2	2/2	2/2
Anterior temporal	1/1	1/1	1/2
Posterior temporal	2/2	2/2	2/3
Dorsal scales at the first ventral	27	27	27
Dorsal scales at neck	23	23	23
Dorsal scales at midbody	23	23	23
Dorsal scales at the third posterior ventral	19	19	19
Dorsal scales before vent	20	19	19
Ventral scales (+ preventral)	134 (+2)	133 (+2)	138 (+1)
Subcaudal scales	42	34	39
Cloacal plate	Divided	Divided	Divided
Gland-like tubercles in the cloacal region	3	0	3
Maxillary teeth	15+2	15+2	16+2
Hemipenis length	8	-	7
Central spot on each ventral	Present	Present	Present
Lateroventral stripe	Present	Present	Present

open-grooved fangs on rear of maxillary bone, (2) rostral without appendages, (3) ventral scales wider than dorsal scales, (4) nasals in contact with each other, (5) dorsal scales smooth, in 23 rows at midbody, (6) first supralabial in contact with loreal, (7) internasal not in contact with loreal, and (9) white or yellow to orange stripe on dorsal scale rows 1–3 only (Murphy and Voris 2014; Köhler et al. 2021). *Myrrophis dakkrongensis* sp. nov. differs from

Myrrophis bennettii by having more dorsal scale rows at midbody (23 vs. 21), more dorsal scale rows before vent (19 or 20 vs. 17 or 15), fewer ventrals (133–138 vs. 158–169), and fewer subcaudals (34–42 vs. 45–56) (Pope 1935; Smith 1943; Murphy and Voris 2014); and from *Myrrophis chinensis* by having more maxillary teeth (15 or 16 + 2 vs. 12 or 13 + 2), the second pair of chin shields small, oblique, and in contact with two infralabials (vs.



Figure 6. Distribution of homalopsid snakes in the genera *Gyiophis*, *Myanophis*, and *Myrrophis* in Indochina and southern China. Data taken from Zhao (2006), Murphy (2007), Karns et al. (2010), Kumar et al. (2012), Quah et al. (2017), Huang (2021), and Köhler et al. (2021).

large, longitudinal, and in contact with 3–4 infralabials) (Fig. 5), and absence of a dorsal pattern (vs. dorsal pattern of black dots arranging in longitudinal series and tending to be concentrated along the middle of the back and on either side of the body) (Boulenger 1896; Pope 1935; Bourret 1936; Smith 1943; Kumar et al. 2012; Murphy and Voris 2014).

Discussion

Gyi (1970) placed 22 of 34 homalopsid species in the genus *Enhydris* with nine species groups. According to, *E. longicauda* was arranged into the *Enhydris (Myrrophis) chinensis* group together with *E. (Myrrophis) bennettii* and *E. (Myrrophis) chinensis* on the basis of the internasal not being in contact with the loreal. In his key to the species and his remarks, Gyi (1970: p. 72 and 106) also stated that the internasal of *E. longicauda* does not

contact the loreal. However, in his description, Gyi (1970: p. 105) stated that the internasal of *E. longicauda* touched the loreal. In fact, in this snake the internasal contacts the loreals (Bourret 1934, 1936; Smith 1943). Hence, Gyi's placement of *E. longicauda* in the *E. (Myrrophis) chinensis* group seems to constitute an error. Current evidence suggests the *Myrrophis chinensis* group consists of three species, including *M. bennettii*, *M. chinensis*, and *M. dakkrongensis* sp. nov.

Based on DNA sequences from a fragment of cyt b (about 1000 bp), Bernstein et al. (2021) supposed that *M. bennettii* and *M. chinensis* were synonymous because of the low genetic divergence (0.0–4.4%) between them and their phylogenetic position on the same clade. Four samples of *M. "bennettii"* used in Bernstein et al. (2021) were collected from Tam Dao, Vinh Phuc Province, northern Vietnam (Vertnet 2023), the same location as three other samples of *M. chinensis*. It seems that Bernstein et al. (2021) did not examine these specimens morphologically because morphological data shown in their Table S3 for *M. "bennettii"* were taken from Karns et al. (2010) and

Kumar et al. (2012). But the positional relationship between loreal and internasal (in contact) of *M. bennettii* shown in Karns et al. (2010) and cited by Bernstein et al. (2021) is in error because true *M. bennettii* actually has the internasal separated from the loreal (Bourret 1936; Smith 1943). Furthermore, *Myrrophis bennettii* inhabits salt water and is known only from southern coastal China and the island of Hainan (Karns et al. 2010; Kumar et al. 2012). In contrast, mainland Tam Dao in Vinh Phuc Province, northern Vietnam, is located about 140 km from the coastal area. Three of these four specimens were named as *M. chinensis* by Bernstein and Ruane (2022: Supplementary Table 1) but subsequently all these four specimens were changed to *M. bennettii* by Bernstein et al. (2023: Appendix S1). Hence, specimens of *M. "bennettii"* used in Bernstein et al. (2021, 2023) and Bernstein and Ruane (2022) should be examined to clarify if they are *M. chinensis*, as suggested by their strong genetic similarity and distance from the coast. In this study, we used a sample of *Myrrophis bennettii* collected from Zhanjiang, Guangdong Province, China (Li et al. 2020) to compare to *M. chinensis* and *M. "bennettii"* genetically. As showed in Table 2, our *M. bennettii* differs from *M. chinensis* as well as from the *M. "bennettii"* of Bernstein et al. (2021, 2023) by 10.1% in DNA sequences. Further, *M. bennettii* also forms an independent clade on the phylogenetic tree (Fig. 1). These results support that *M. bennettii* and *M. chinensis* are distinct species. Recent molecular studies using multilocus marker system (Li et al. 2020) and DNA barcoding (Wu et al. 2023) also reject the hypothesis that *M. bennettii* and *M. chinensis* are conspecific.

The distributional range of the *Gyiophis-Myanophis-Myrrophis* clade is scattered (Fig. 6). Each of *Gyiophis salweenensis*, *G. vorisi*, and *Myanophis thanlyinensis* occurs in a single location in Myanmar within fresh water habitats (Murphy 2007; Quah et al. 2017; Köhler et al. 2021). *Myrrophis bennettii* occurs in southern China and inhabits brackish and salt water (Smith 1943; Zhao 2006; Kumar et al. 2012; Huang 2021). *Myrrophis chinensis* occurs in southern China and northern Vietnam and can be found in fresh, brackish, and salt water (Smith 1943; Zhao 2006; Karns et al. 2010; Huang 2021). The distributional ranges of *M. bennettii* and *M. chinensis* overlap in the coastal area of southern China (Kumar et al. 2012). *Myrrophis dakkrongensis* sp. nov. occurs in upper reaches of the Dak Krong River in southern Vietnam. This river system originates from Dak Nong and Dak Lak provinces and is confluent with the Mekong River via the Tonle Srepok River in Cambodia. The Dak Krong River is independent from other river systems and coastal areas in the north that are inhabited by two congeners. *Myrrophis dakkrongensis* sp. nov. is currently known only from its type locality in Dak Nong Province, but it is expected to occur in other places within the Dak Krong basin.

Our tree (Fig. 1), which is a matrilineal genealogy, raises a taxonomic concern because it depicts paraphyly with respect to *Gyiophis-Myanophis-Myrrophis*, and *Myrrophis* itself is not retrieved as monophyletic, but forms three independent clades corresponding to two described

species and the new species; *Gyiophis* and *Myanophis* cluster together as sister taxa. The absence of monophyly in *Myrrophis* is quite surprising given the low ratio of species to genera in homalopsid snakes. This taxonomic splitting can obscure historical relationships among species. One solution is to erect new genera for two species of *Myrrophis*, but doing so would obscure phylogenetic relationships. That said, our tree was reconstructed using maternally inherited mtDNA sequences only and this may not be consistent with a nDNA phylogeny given that mito-nuclear discordance is quite commonly detected, and in this case it would most likely involves the introgression of mitogenomes as a consequence of hybridization (e.g., Platt et al. 2018; Tamashiro et al. 2019; Kimball et al. 2021). Another solution is to lump the six species belonging to these three genera into *Myrrophis*, which has priority by date of publication. This arrangement better reflects historical relationships than the current taxonomy, which has genera with one or two species only. Thus, further phylogenetic studies using nuclear DNA sequences from our new species and all other taxa in the *Gyiophis-Myanophis-Myrrophis* clade are needed to clarify if such discordance exists and resolve the taxonomic concern within the clade.

Acknowledgements

Technical support from the Molecular Biodiversity Research Laboratory (Hanoi National University, Vietnam) is gratefully acknowledged. We would like to thank Dr. Le Thi Chau and Dr. Nguyen Thi Phuong Mai (TNISR) for arranging documents for the field trip; the board of Nam Nung NR and Dak Nong Department of Agriculture and Rural Development for their permissions to work in the field; brothers in Forest Station No. 8 (Nam Nung NR) for their help in the field; and three reviewers (Fred Kraus, Gunther Köhler, and Bryan Stuart) and editor for greatly improving the earlier version of the manuscript. This research is funded by the Vietnam National Foundation for Science and Technology Development (NAFOSTED) under grant number 106.05-2021.69 and partly by PIFI Visiting Scientist program of Chinese Academy of Sciences (CAS) (2024VBB0017), Southeast Asia Biodiversity Research Institute, CAS, and the Animal Branch of the Germplasm Bank of Wild Species, CAS (the Large Research Infrastructure Funding).

References

- Alfaro ME, Karns DR, Voris HK, Brock CD, Stuart BL (2008) Phylogeny, evolutionary history, and biogeography of Oriental-Australian rear-fanged water snakes (Colubroidea: Homalopsidae) inferred from mitochondrial and nuclear DNA sequences. Molecular Phylogenetics and Evolution 46: 576–593. <https://doi.org/10.1016/j.ympev.2007.10.024>
- Berstein JM, Murphy JC, Voris HK, Brown RM, Ruane S (2021) Phylogenetics of mud snakes (Squamata: Serpentes: Homalopsidae): A paradox of both undescribed diversity and taxonomic inflation. Molecular Phylogenetics and Evolution 160: 107109. <https://doi.org/10.1016/j.ympev.2021.107109>
- Bernstein JM, Ruane S (2022) Maximizing molecular data from low-quality fluid-preserved specimens in natural history collec-

- tions. *Frontiers in Ecology and Evolution* 10: 893088. <https://doi.org/10.3389/fevo.2022.893088>
- Bernstein JM, de Souza HF, Murphy JC, Voris HK, Brown RM, Myers E.A, Harrington S, Shanker K, Ruane S (2023) Phylogenomics of fresh and formalin specimens resolves the systematics of Old World mud snakes (Serpentes: Homalopsidae) and expands biogeographic inference. *Bulletin of the Society of Systematic Biologists* 2: 1–24. <https://doi.org/10.1806/bssb.v2i1.9393>
- Boulenger GA (1896) Catalogue of the Snakes in the British Museum (Natural History). Volume III, Containing the Colubridae (Opisthoglyphae and Proteroglyphae), Amblycephalidae, and Viperidae. British Museum (Natural History), London, 727 pp. <https://doi.org/10.5962/bhl.title.8316>
- Bourret R (1934) Notes herpétologiques sur l'Indochine Française IV. Sur une collection d'Ophidiens de Cochinchine et du Cambodge. *Bulletin Générale de l'Instruction Publique* 1934: 13–30.
- Bourret R (1936) Les Serpents de l'Indochine. Tome II. Catalogue systématique descriptif. Imprimerie Henri Basuyau & Cie, Rue des Riegans, Toulouse, 505 pp.
- Dowling HG (1951) A proposed standard system of counting ventrals in snakes. *British Journal of Herpetology* 1: 97–99.
- Dowling HG, Savage JM (1960) A guide to the snake hemipenis: A survey of basic structure and systematic characteristics. *Zoologica* 45: 17–28. <https://doi.org/10.5962/p.203350>
- Gyi KK (1970) A revision of colubrid snakes of the subfamily Homalopsinae. University of Kansas Publications, Museum of Natural History, Lawrence 20: 47–223.
- Hillis DM, Bull JJ (1993) An empirical test of bootstrapping as a method for assessing confidence in phylogenetic analysis. *Systematic Biology* 42: 182–192. <https://dx.doi.org/10.1093/sysbio/42.2.182>
- Hoang DT, Chernomor O, von Haeseler A, Minh BQ, Vinh LS (2018) UFBoot2: Improving the ultrafast bootstrap approximation. *Molecular Biology and Evolution* 35: 518–522. <https://doi.org/10.1093/molbev/msx281>
- Huang S (2021) *Sinoophis: Atlas of Snakes in China*, Volumes I and II. The Straits Publishing, Fuzhou, 284 pp. + 645 pp. [in Chinese].
- Indahsari LIN, Fatchiyah F, Kurniawan N (2019) DNA barcoding as a method for species identification: Case study in *Ahaetulla* snake. *Journal of Physics: Conference Series* 1374: 012011. <https://doi.org/10.1088/1742-6596/1374/1/012011>
- Karns DR, Lukoschek V, Osterhage J., Murphy JC, Voris HK (2010) Phylogeny and biogeography of the *Enhydris* clade (Serpentes: Homalopsidae). *Zootaxa* 2452: 18–30.
- Kimball RT, Guido M, Hosner PA, Braun EL (2021) When good mitochondria go bad: Cyto-nuclear discordance in landfowl (Aves: Galliformes). *Gene* 801: 145841. <https://doi.org/10.1016/j.gene.2021.145841>
- Köhler G, Khaing KPP, Than NL, Baranski D, Schell T, Greve C, Janke A, Pauls SU (2021) A new genus and species of mud snake from Myanmar (Reptilia, Squamata, Homalopsidae). *Zootaxa* 4915: 301–325. <https://doi.org/10.11646/zootaxa.4915.3.1>
- Kumar AB, Sanders KL, George S, Murphy JC (2012) The status of *Eurostus dussumieri* and *Hypsirhina chinensis* (Reptilia, Squamata, Serpentes): With comments on the origin of salt tolerance in homalopsid snakes. *Systematics and Biodiversity* 10: 479–489. <https://doi.org/10.1080/14772000.2012.751940>
- Li J, Liang D, Wang Y, Guo P, Huang S, Zhang P (2020) A large-scale systematic framework of Chinese snakes based on a unified multi-locus marker system. *Molecular Phylogenetics and Evolution* 148: 106807. <https://doi.org/10.1016/j.ympev.2020.106807>
- Minh Q, Nguyen MAT., von Haeseler A (2013) Ultrafast approximation for phylogenetic bootstrap. *Molecular Biology and Evolution* 30: 1188–1195. <https://doi.org/10.1093/molbev/mst024>
- Murphy JC (2007) A review of *Enhydris maculosa* (Blanford, 1879) and the description of a related species (Serpentes, Homalopsidae). *Hamadryad* 31: 281–287.
- Murphy JC, Voris HK (2014) A checklist and key to the homalopsid snakes (Reptilia, Squamata, Serpentes), with the description of new genera. *Fieldiana: Life and Earth Sciences* 8: 1–43.
- Murphy JC, Lang RD, Gower DJ, Sanders KL (2012) The Moluccan short-tailed snakes of the genus *Brachyorrhos* Kuhl (Squamata: Serpentes: Homalopsidae), and the status of *Calamophis* Meyer. *The Raffles Bulletin of Zoology* 60: 501–514.
- Nguyen LT, Schmidt HA, von Haeseler A, Minh BQ (2015) IQ-TREE: A fast and effective stochastic algorithm for estimating maximum likelihood phylogenies. *Molecular Biology and Evolution* 32: 268–274. <https://doi.org/10.1093/molbev/msu300>
- Nylander JAA (2004) MrModeltest v2. Program distributed by the author. Evolutionary Biology Centre, Uppsala University.
- Platt RN, Faircloth BC, Sullivan KA, Kieran TJ, Glenn TC, Vandewege MW, Lee TE, Baker RJ, Stevens RD, Ray DA (2018) Conflicting evolutionary histories of the mitochondrial and nuclear genomes in new world *Myotis* bats. *Systematic Biology* 67: 236–249. <https://doi.org/10.1093/sysbio/syx070>
- Pope CH (1935) The Reptiles of China. Vol. X. Natural History of Central Asia. The American Museum of Natural History, New York, xliii + 604 pp., pls. 1–27.
- Quah ESH., Grismer LL, Wood PR, Thura MK, Zin T, Kyaw H, Lwin N, Grismer, MS, Murdoch ML (2017) A new species of mud snake (Serpentes, Homalopsidae, *Gyiophis* Murphy & Voris, 2014) from Myanmar with a first molecular phylogenetic assessment of the genus. *Zootaxa* 4238: 571–582. <https://doi.org/10.11646/zootaxa.42-38.4.5>
- Ronquist RR, Huelsenbeck JP (2003) MrBayes 3: Bayesian phylogenetic inference under mixed models. *Bioinformatics* 19: 1572–1574. <https://doi.org/10.1093/bioinformatics/btg180>
- Simmons JE (2002) Herpetological collecting and collections management. Revised edition. Society for the Study of Amphibians and Reptiles, *Herpetological Circular* 31: 1–153.
- Smith MA (1943) The Fauna of British India, including Ceylon and Burma. Reptilia and Amphibia. Taylor and Francis, London, 583 pp.
- Tamura K, Peterson D, Peterson N, Stecher G, Nei M, Kumar S (2011) MEGA5: Molecular Evolutionary Genetics Analysis using maximum likelihood, evolutionary distance, and maximum parsimony methods. *Molecular Biology and Evolution* 28: 2731–2739. <https://dx.doi.org/10.1093/molbev/msr121>
- Tamashiro RA, White D., Braun MJ, Faircloth BC, Braun EL, Kimball RT (2019) What are the roles of taxon sampling and model fit in tests of cyto-nuclear discordance using avian mitogenomic data? *Molecular Phylogenetics and Evolution* 130: 132–142. <https://doi.org/10.1016/j.ympev.2018.10.008>
- Thompson JD, Higgins DG & Gibson TJ (1994) CLUSTAL W: Improving the sensitivity of progressive multiple sequence alignment through sequence weighting, position-specific gap penalties and weight matrix choice. *Nucleic Acids Research* 22: 4673–4680. <https://doi.org/10.1093/nar/22.22.4673>
- Trifinopoulos J, Nguyen LT, von Haeseler A, Minh BQ (2016) W-IQ-TREE: A fast online phylogenetic tool for maximum likelihood analysis. *Nucleic Acids Research* 44: W232–W235. <https://doi.org/10.1093/nar/gkw256>

- Uetz P, Freed P, Hosek J (Eds.) (2023) The Reptile Database. Available from: <http://www.reptile-database.org> (accessed 21 August 2023).
- Vernet (2023) <http://www.vertnet.org/index.html>. Version 2016-09-29 (accessed 28 October 2023)
- Wu YH, Hou SB, Yuan ZY, Jiang K, Huang RY, Wang K, Liu Q, Yu ZB, Zhao HP, Zhang BL, Chen JM, Wang LJ, Stuart BL, Chambers EA, Wang YF, Gao W, Zou DH, Yan F, Zhao GG, Fu ZX, Wang SN, Jiang M, Zhang L, Ren JL, Wu YY, Li JT, Zhao WG, Murphy RW,
- Huang S, Guo P, Zhang YP, Che J (2023) DNA barcoding of Chinese snakes reveals hidden diversity and conservation needs. *Molecular Ecology Resources* 23: 1124–1141. <https://doi.org/10.1111/1755-0998.13784>
- Zhao E (2006) Snakes of China. Vol. II. Anhui Science and Technology Publishing House, Hefei, Anhui, Vol. I, 372 pp., 280 pp. [in Chinese].

Appendix 1

Specimens examined (n = 31)

Enhydris enhydris, 3 specimens: ITBCZ 7699, 7724, 7725 (Ta Kou, Binh Thuan, Vietnam).

Enhydris innominata, 3 specimens: ITBCZ 8383, 8384, 8386 (Thanh Hoa, Long An, Vietnam).

Enhydris longicauda, 3 specimens: ITBCZ 8386, 8413, 8414 (Mekong Delta, purchased in a local market in Long An Province, Vietnam).

Enhydris subtaeniata, 4 specimens: ITBCZ 7447–9 (Son Ha, Quang Ngai, Vietnam); ITBCZ 8382 (My Phuoc Tay, Tien Giang, Vietnam).

Hypsiscopus murphyi, 5 specimens: ITBCZ 176, 177 (Nui Chua, Ninh Thuan, Vietnam), 7444–6 (Son Tinh, Quang Ngai, Vietnam).

Myrophis chinensis, 13 specimens: ROM 25377–85 (Hanoi, Vietnam); ROM 30889, 30890, 31031, 41565 (Tam Dao, Vinh Phuc, Vietnam).